

# Lawrence Berkeley National Laboratory

## LBL Publications

### Title

Refined model of the oxidation states and the structures of the Mn/Ca/Cl cluster of the oxygen evolving complex of photosystem II

### Permalink

<https://escholarship.org/uc/item/7gw876m5>

### Authors

Yachandra, VK

Cinco, RM

Robblee, JH

et al.

### Publication Date

2023-12-11

Peer reviewed

*Photosynthesis: Mechanisms and Effects* (Garab, G., ed.) Kluwer Academic Publishers, The Netherlands, (1998) 1273-1278.

## **REFINED MODEL OF THE OXIDATION STATES AND STRUCTURES OF THE Mn/Ca/Cl CLUSTER OF THE OXYGEN EVOLVING COMPLEX OF PHOTOSYSTEM II.**

Roehl M. Cinco<sup>1,2</sup>, Carmen Fernandez<sup>1,2</sup>, Johannes Messinger<sup>1</sup>, John H. Robblee<sup>1,2</sup>, Henk Visser<sup>1,2</sup>, Karen L. McFarlane<sup>1</sup>, Uwe Bergmann<sup>1</sup>, Pieter Glatzel<sup>1,3</sup>, Stephen P. Cramer<sup>1,3</sup>, Kenneth Sauer<sup>1,2</sup>, Melvin P. Klein<sup>1</sup> and Vittal K. Yachandra<sup>1</sup>.  
<sup>1</sup>*Physical Biosciences Division, Lawrence Berkeley National Laboratory*, <sup>2</sup>*Department of Chemistry, University of California, Berkeley, CA 94720*, and <sup>3</sup>*Department of Applied Physics, University of California, Davis, CA 95616*.

*Key Words:* photosystem 2, X-ray spectroscopy, manganese cluster, O<sub>2</sub>-evolution, S-states

### **1. Introduction**

Central to the problem of photosynthetic oxygen evolution is the structure and function of the Mn/Ca/Cl complex that appears to be the locus of charge accumulation and water splitting. In the recent past our group has presented a topological model for the structure of the tetranuclear Mn cluster, the oxidation state assignments of the S-states of the Kok cycle, the orientation of the Mn-Mn vectors relative to the membrane normal, and evidence for the proximity of Ca to the Mn (1-3).

In this paper we present refinements to the previously proposed structure. Direct evidence for the proximity of Ca to Mn, and the first evidence for Cl being a ligand to Mn are provided. Structural changes on the advancement from S<sub>2</sub> to S<sub>3</sub> and also on the S<sub>0</sub> to S<sub>1</sub> transformation have been determined. The relative orientations of the Mn-cofactor vectors are inferred.

Additionally, we confirm the oxidation state changes and assignments vs. S-states that we had offered earlier based on Mn K-edge spectra (3) by high resolution Mn K $\beta$  fluorescence spectroscopy. By comparison of the XANES of oriented samples in the S<sub>2</sub> and S<sub>3</sub> states we confirm the absence of Mn oxidation in the S<sub>2</sub> to S<sub>3</sub> transition.

### **2. Materials and Methods**

PS II membrane sample preparation has been described previously (1, 2). The paper by Fernandez et al. in this volume gives the procedures for Sr incorporation, for flash advancing the samples through the several S-states, and for orienting the membranes. The paper by Messinger et al. in this volume gives the procedures for preparing the physiological S<sub>0</sub> state samples. X-ray absorption spectroscopic methods have been described previously. The correlation of high resolution Mn K $\beta$  fluorescence spectra with Mn oxidation state has been reported previously (4).

### 3. Oxidation States vs. S-states

Roelofs et al. (3) demonstrated that flash advanced PS II samples prepared from spinach exhibited XANES spectra that showed Mn oxidation on going from  $S_0$  to  $S_1$  and from  $S_1$  to  $S_2$  but no further oxidation during the  $S_2$  to  $S_3$  transition, confirming our earlier report (5).

Preliminary studies using high resolution X-ray fluorescence spectroscopy have confirmed these data. In this technique, the energy of the Mn  $K\beta$  emission is measured with a high resolution dispersive spectrometer. The shape and energy position of the  $K\beta_{1,3}$  emission reflects the oxidation state(s) of the emitting Mn atom(s). The emission occurs from a 3p level that is mainly influenced by the number of unpaired 3d electrons, and it is less sensitive to the symmetry and bonding than the K-edge absorption which involves transitions to the 4p level. Studies on model compounds demonstrate that Mn(II) complexes appear at higher energy while those of Mn(III) and Mn(IV) occur at lower energy (4).

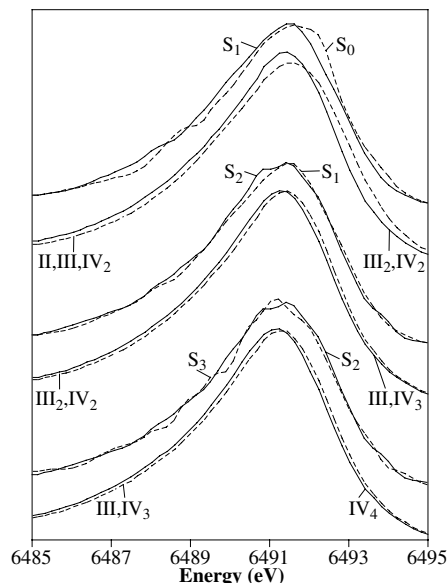


Figure 1. High resolution Mn  $K\beta$  X-ray fluorescence spectra of PS II in the  $S_0$ ,  $S_1$ ,  $S_2$  and  $S_3$  states and simulated spectra for mixtures of Mn model complexes reflecting the oxidation states (II,III,IV<sub>2</sub>), (III<sub>2</sub>,IV<sub>2</sub>), (III,IV<sub>3</sub>) and (IV<sub>4</sub>).

Figure 1 shows Mn emission spectra from PS II samples in the  $S_0$ ,  $S_1$ ,  $S_2$  and  $S_3$  states and a series of simulated spectra. It is apparent that there is a difference between the  $S_0$  and  $S_1$  states and between the  $S_1$  and  $S_2$  states. There is virtual superposition between the  $S_2$  and  $S_3$  state sample spectra. First moment analysis shows that there is a shift of  $\sim 0.1$  eV in progressing from the  $S_0$  to  $S_1$  state,  $\sim 0.05$  eV from the  $S_1$  to  $S_2$ , and negligible shift from the  $S_2$  to  $S_3$  state. A comparison to the model compound spectra suggests that these changes correspond to a Mn(II) to Mn(III) oxidation during the  $S_0$  to  $S_1$  transition, and a Mn(III) to Mn(IV) oxidation during the  $S_1$  to  $S_2$  transition. The absence of a shift in the  $S_2$  to  $S_3$  transition indicates a lack of Mn oxidation.

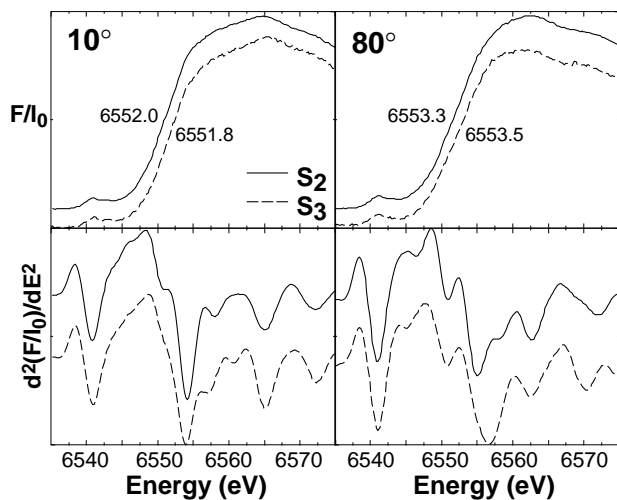


Figure 2. Mn K-edge spectra and second derivatives for  $S_2$  and  $S_3$  samples with the membrane normal at  $10^\circ$  and  $80^\circ$  orientation to the X-ray  $E$ -vector. The inflection point energies (in eV) for the  $S_2$  and  $S_3$  states are shown in the top panels.

Highly oriented PS II membranes in both  $S_2$  and  $S_3$  states have been prepared for performing XAS dichroism experiments. Figure 2 shows the XANES region for two orientations of samples in the  $S_2$  and  $S_3$  states. It is evident that at each orientation there is virtual

identity in the absorption edge energies and shapes between the two S-states which confirms the results from isotropic PS II samples. Hence, we offer these data to further demonstrate that there is no Mn oxidation on advance from S<sub>2</sub> to S<sub>3</sub>.

In summary, we conclude that the oxidation state assignment for samples in the S<sub>0</sub>, S<sub>1</sub>, S<sub>2</sub> and S<sub>3</sub> states is respectively (II,III,IV<sub>2</sub>) or (III<sub>3</sub>,IV), (III<sub>2</sub>,IV<sub>2</sub>), (III,IV<sub>3</sub>) and (III,IV<sub>3</sub>)\* where the \* represents an oxidized species other than Mn. Histidyl, tyrosyl or oxyl radicals are likely candidates (2, 5, 6). Figure 3 summarizes the suggested oxidation state assignments vs. S-states of the Kok cycle.

#### 4. Structure of the Manganese Cluster

Previously, we have reported a hypothetical structure topologically consistent with the Mn EXAFS data (1). That "dimer of dimers" structure is based on the consistency of structural motifs known from the synthetic Mn coordination chemistry literature: di- $\mu$ -oxo bridged binuclear Mn units with 2.7 Å Mn-Mn spacing and  $\mu$ -oxo- and carboxylato-bridged units with 3.3 Å Mn-Mn spacing. We also suggested a Mn-Ca(Sr) interaction at ~ 3.5 Å (7). No significant structural changes have been observed between samples in the untreated S<sub>1</sub> and S<sub>2</sub> states. Inhibition by both F<sup>-</sup> and NH<sub>3</sub>, as well as generation of the *g*=4.1 EPR signal, removes the degeneracy between the two 2.7 Å units in these S<sub>2</sub> states. X-ray dichroism of oriented samples in the S<sub>1</sub>, S<sub>2</sub> and ammonia treated S<sub>2</sub> states established the relative orientations of the Mn-Mn vectors relative to the membrane normal (8-10).

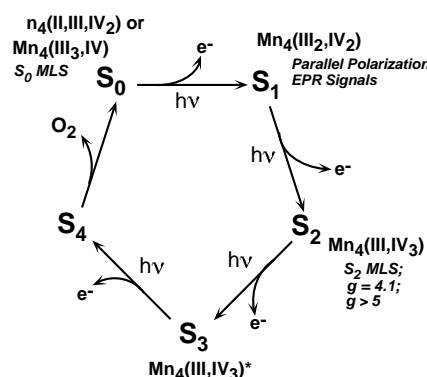


Figure 3. Manganese oxidation states and corresponding EPR signals for each S-state in the Kok cycle.

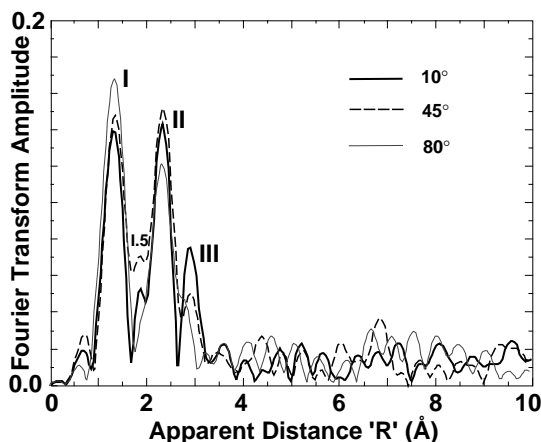


Figure 4. Fourier transforms of Mn EXAFS spectra of S<sub>3</sub> samples with the membrane normal oriented at 10°, 45°, and 80° to the X-ray E-vector. The peak labelled I.5 is attributed to backscattering from Cl.

EXAFS data from oriented S<sub>3</sub> samples are shown in Figure 4. It is evident that the Fourier features are highly dichroic. Fits to the data show that both of the shorter Mn-Mn distances have increased, one to 2.8 Å and the second to nearly 3.0 Å. This is schematically represented in Figure 5. The orientations of these Mn-Mn vectors can be obtained from these data and such analysis is currently underway.

Very significantly, a new feature labelled I.5 in Figure 4 appears between the first two larger Fourier peaks labelled I and II in the 10° S<sub>3</sub> spectrum. Extensive analysis has been performed with the aim of identifying the element responsible for this backscattering feature. It does not fit well to low-Z elements such as C, O or N. It fits exceedingly well to a single Cl at 2.2 Å. The Mn EXAFS spectra of synthetic Mn complexes with terminal Mn-Cl bonds exhibit features identical to that shown here (see the accompanying paper by Fernandez et

al. in this volume). The clarity of the new feature and analyses of the  $S_3$  data are aided by the lengthening of the second shell of Mn-Mn vectors. We believe this to be the first direct physical evidence for the ligation of Cl to Mn in the OEC. Determination of the direction of the Mn-Cl vector is in progress.

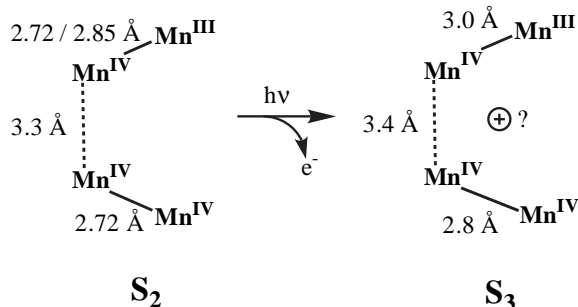


Figure 5. Mn-Mn bond lengths depicted for the  $S_2$  and  $S_3$  states of the OEC. The two Mn<sup>IV</sup>-Mn<sup>III</sup> bond distances given are for the MLS and  $g=4.1$  forms of the  $S_2$  state, respectively.

Although this new feature is self evident in the  $S_3$  data, comparative re-analysis of data from oriented  $S_2$  samples that includes Cl in the Mn coordination sphere at 2.2 Å improves the quality of the fits.

Changes within the Mn cluster between the  $S_0$  and  $S_1$  states are reported in the present volume in the paper by Messinger et al. (11).

There has been considerable controversy over the question of whether there is a Ca atom proximal to the Mn cluster. We have presented comparative evidence from Mn EXAFS of native Ca containing PS II membranes and from those in which Ca was replaced by Sr. The Fourier peak (at an apparent distance of  $\sim 3$  Å) showed increased intensity upon Sr replacement, as is expected for a higher Z element. The best simulations incorporated Mn at 3.3 Å and Sr at 3.5 Å (7).

To address more directly the question of Ca(Sr) proximity to Mn, we have performed Sr EXAFS on samples in which Ca was replaced by Sr. The samples used were treated to remove all but the functional Sr (12, 13).

The accompanying paper by Fernandez et al. shows the Sr EXAFS Fourier transforms of an intact isotropic PS II sample and that of a sample to which  $\text{NH}_2\text{OH}$  had been added. The spectrum of the intact sample exhibits a feature at an apparent distance of 3 Å. The spectrum of the  $\text{NH}_2\text{OH}$  treated sample shows that feature to be absent.  $\text{NH}_2\text{OH}$  is known to disrupt the Mn cluster and a sample so treated serves as a control to demonstrate that the Sr is within 3.5 Å of Mn.

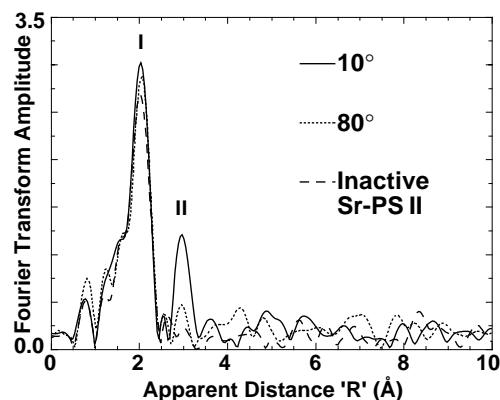


Figure 6. Fourier transforms of Sr-EXAFS spectra of Sr-reconstituted PS II samples of active Sr-PS II oriented with the membrane normal at 10° (solid line), and at 80° (dotted line) with respect to the X-ray E-vector, and inactivated Sr-PS II (dashed line).

Figure 6 shows the Fourier transform of the Sr EXAFS for two orientations of highly oriented PS II membranes containing one or fewer Sr/4Mn. It is apparent that the second feature, best simulated by two Sr-Mn interactions, is highly dichroic. Although full analysis of this feature is incomplete, we are able to infer that the direction of the 3.5 Å

Sr-Mn vectors are roughly along the membrane normal. Hence we believe these data are definitive evidence for the proximity of Ca(Sr) to Mn.

We point out that a Mn-O-Ca-O-Mn bridge provides a pathway, albeit weak, for magnetic coupling within the cluster that may help our understanding of the EPR of the OEC (14).

## 5. Refinement of the Mn/Ca/Cl model

Figure 7 shows the refined model for the Mn cluster. In this version we have added a second Mn - Ca interaction at  $\sim 3.5$  Å and shown these vectors as approximately along the membrane normal. Moreover, we have added a Cl ligand at  $\sim 2.2$  Å from Mn, this vector also roughly along the membrane normal. Finally, we include an histidine whose presence was established by ESEEM spectroscopy (15). We emphasize that this model is *topologically* correct in that the directions of the individual vectors are only determined on a cone of revolution about the membrane normal; we cannot assign histidine or Cl ligation or Mn-Ca interactions to specific Mn atoms. Other arrangements are possible and some have been presented elsewhere (16).

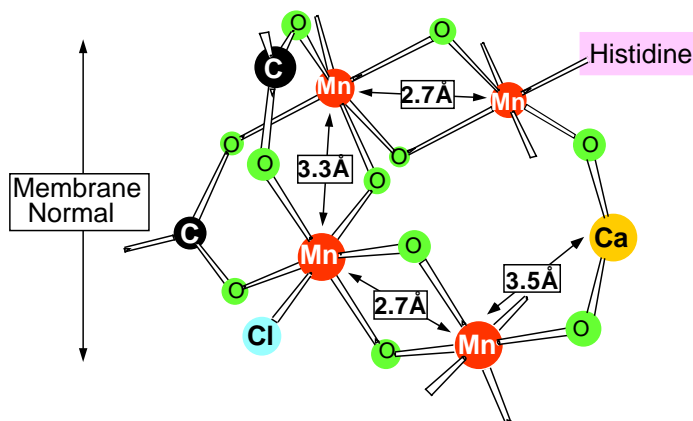


Figure 7. Proposed structure of the Mn cluster in the Oxygen Evolving Complex of Photosystem II including the Ca and Cl cofactors.

## 6. Mechanistic Implications

The new measurements that confirm the absence of Mn oxidation on advance from the  $S_2$  to the  $S_3$  state remain consistent with one mechanism of oxygen evolution previously suggested by us (2). They require, however, reevaluation of other suggested mechanisms that invoke specifically Mn oxidation on each step of the Kok cycle.

The increase in the lengths of the Mn-Mn distance from about  $2.7$  Å to  $2.8$  Å and  $2.9$ - $3.0$  Å during the  $S_2$  to  $S_3$  transition reflects significant rearrangements within the Mn cluster as do the changes from the  $S_0$  to  $S_1$  states. Such changes must be addressed in future suggested mechanisms.

Establishing the presence of both Ca and Cl proximal to the Mn cluster explains the earlier observations that their presence is essential for traversing the Kok cycle. The presence of these essential cofactors will require new ideas on their roles and functions.

## 7. Acknowledgments

This research was supported by the National Institutes of Health (GM55302), and the Director, Office of Basic Energy Sciences, Division of Energy Biosciences of the U.S. Department of Energy (DOE), under Contract DE-AC03-76SF00098. C. F. was supported by a fellowship from FAPESP, and J. M. was partly supported by a DFG

grant (Me 1629/1-1). We are grateful to Profs. G. Christou, W. H. Armstrong, V. L. Pecoraro, K. Wieghardt and J.-J. Girerd for generously providing us with the Mn model compounds. Synchrotron radiation facilities were provided by the Stanford Synchrotron Radiation Laboratory (SSRL) which is operated by the Department of Energy, Office of Basic Energy Sciences. The SSRL Biotechnology Program is supported by the National Institutes of Health, National Center of Research Resources, Biomedical Technology Program, and by the Department of Energy, Office of Health and Environmental Research.

## References

- 1 Yachandra, V. K., DeRose, V. J., Latimer, M. J., Mukerji, I., Sauer, K. and Klein, M. P. (1993) *Science*, 260, 675-679.
- 2 Yachandra, V. K., Sauer, K. and Klein, M. P. (1996) *Chem. Rev.* 96, 2927-2950.
- 3 Roelofs, T. A., Liang, W., Andrews, J. C., Cinco, R., Dau, H., Rompel, A., Andrew, J. C., Yachandra, V. K., Sauer, K. and Klein, M.P. (1996) *Proc. Nat'l. Acad. Sci. U. S. A.*, 93, 3335-3340.
- 4 Peng, G., DeGroot, F. M. F., Hamäläinen, K., Moore, J. A., Wang, X., Grush, M. M., Hastings, J. B., Siddons, D. P., Armstrong, W. H., Mullins, O. C. and Cramer, S. P. (1994) *J. Am Chem. Soc.* 116, 2914-2920.
- 5 Guiles, R. D., Zimmermann, J.-L., McDermott, A. E., Yachandra, V. K., Cole, J. L., Dexheimer, S. L., Britt, R. D., Wieghardt, K., Bossek, U., Sauer, K. and Klein, M. P. (1990) *Biochemistry*, 29, 471-485.
- 6 Boussac, A., Zimmermann, J.-L., Rutherford, A. W., and Lavergne, J. (1990) *Nature* 347, 303-306.
- 7 Latimer, M. J., DeRose, V. J., Mukerji, I., Yachandra, V. K., Sauer, K. and Klein, M. P. (1995) *Biochemistry*, 34, 10898-10909.
- 8 DeRose, V. K., Latimer, M. J., Zimmermann, J.-L., Mukerji, I., Sauer, K., Yachandra, V. K. and Klein, M. P. (1995) *Chem. Phys. (J. Amesz and A. J. Hoff, eds)* 194, 443-459.
- 9 Mukerji, I., Andrews, J. C., DeRose, V. J., Latimer, M. J., Yachandra, V. K., Sauer, K. and Klein, M. P. (1994) *Biochemistry*, 33, 9712- 9721.
- 10 Dau, H., Andrews, J. C., Yachandra, V. K., Roelofs, T. A., Latimer, M. J., Liang, W., Sauer, K., Yachandra, V. K. and Klein, M. P. (1995) *Biochemistry*, 34, 5274-5287.
- 11 Messinger, J., Robblee, J. H., Fernandez, C., Cinco, R. M., Visser, H., Bergmann, U., Cramer, S. P., Campbell, K. A., Peloquin, J. M., Britt, R. D., Sauer, K., Yachandra, V. K. and Klein, M. P. (This volume).
- 12 Fernandez, C., Cinco, R. M., Robblee, J. H., Messinger, J., Pizarro, S., Sauer, K., Klein, M. P. and Yachandra, V. K. (This volume).
- 13 Cinco, R. M., Robblee, J. H., Rompel, A., Fernandez, C., Yachandra, V. K., Sauer, K. and Klein, M. P. (1998) *J. Phys. Chem.* (in press).
- 14 Blondin, G. and Girerd, J.-J. (Personal communication).
- 15 Tang X.,-S, Diner, B. A., Larsen, B. S., Gilchrist, M. L. Jr, Lorigan, G. A. and Britt, R. D. (1994) *Proc Nat'l. Acad. Sci. U. S. A.* 91, 704-708.
- 16 DeRose, V. J., Mukerji, I., Latimer, M. J., Yachandra, V. K., Sauer, K. and Klein, M. P. (1994) *J. Am Chem. Soc.* 116, 5239-5249.